Failure of single-parameter scaling of wave functions in Anderson localization

S.L.A. de Queiroz*
Instituto de Física, Universidade Federal do Rio de Janeiro,
Caixa Postal 68528, 21945-970 Rio de Janeiro RJ, Brazil
(Dated: 1st February 2008)

We show how to use properties of the vectors which are iterated in the transfer-matrix approach to Anderson localization, in order to generate the statistical distribution of electronic wavefunction amplitudes at arbitrary distances from the origin of $L^{d-1} \times \infty$ disordered systems. For $d = 1$ our approach is shown to reproduce exact diagonalization results available in the literature. In $d = 2$, where strips of width $L \leq 64$ sites were used, attempted fits of gaussian (log-normal) forms to the wavefunction amplitude distributions result in effective localization lengths growing with distance, contrary to the prediction from single-parameter scaling theory. We also show that the distributions possess a negative skewness S, which is invariant under the usual histogram-collapse rescaling, and whose absolute value increases with distance. We find $0.15 \lesssim -S \lesssim 0.30$ for the range of parameters used in our study.

PACS numbers: PACS numbers: 71.23.An, 73.20.Fz

I. INTRODUCTION

The localization model introduced by Anderson[1] incorporates two basic elements, namely the rules of quantum mechanics applied to a single-electron, tight-binding model Hamiltonian, plus quenched disorder (realized, e.g., by assigning random self-energies to lattice sites). Its original purpose was to show the existence of a disorder-induced transition in three-dimensional systems, from metallic (diffusive) to insulating (localized) electronic behavior, upon increasing randomness. Over the years the model has turned out to exhibit a rich variety of physical aspects, many of them highlighted by the (single–parameter) scaling theory of localization (SPST)[2,3]. Of particular interest here is the fact that, in zero magnetic field and in the absence of spin-orbit couplings, SPST predicts insulating behavior, for any finite amount of disorder, in spatial dimensions $d = 1$ and 2, though in the marginal case $d = 2$ one has borderline phenomena such as weak localization. Interest in the Anderson transition has been renewed by reports of metallic behavior in dilute two-dimensional electron-hole systems[4]. While phenomenological, percolation-based theories have been able to reproduce experimentally-observed trends in some detail[5], attempts to reconcile basic theoretical assumptions to experimental evidence have only met limited success so far. For instance, numerical evidence has been produced[6] against the idea that electron-electron interactions (not included in scaling theory) might play a role in driving the two-dimensional transition[4].

Even when one confines oneself to the original Anderson picture of non-interacting electrons in three-dimensional lattices, where the existence of a transition is not questioned, progress towards extracting reliable numerical estimates of critical quantities has been remarkably hard[7,8,9,10,11,12,13]. Recently, systematic consideration of irrelevant variables and non-linear corrections to single-parameter scaling[14,15,16,17,18,19] has helped produce results with a fairly reasonable claim to consistently narrow error bars.

It is thus of interest to reexamine the basic methods which have been used in the past 20 years, in conjunction with SPST, to study the Anderson localization problem. A step in this direction has been given in Ref. 20, whose authors obtained wave functions via exact diagonalization, for both one-dimensional and finite, $L \times L$, two-dimensional systems. By averaging over randomness, they obtained probability distributions of wavefunction amplitudes on sites at varying distances from an arbitrary origin. Such distributions were compared to predictions from SPST; though agreement was good in $d = 1$, the two-dimensional results were in contradiction to the idea of a single localization length depending only on disorder intensity: instead, a clear logarithmic increase with distance, at fixed disorder, was found from their fits for that quantity.

In Ref. 20, finite-size effects were avoided in $d = 2$ by considering disorder strengths such that the corresponding localization length, as predicted by single-parameter theory, is $\lambda \lesssim 10$ (see, e.g., Refs. 7,9), and using suitably large systems with $L = 300$. On the other hand, numerous studies of the Anderson transition are set up on quasi-one dimensional geometries, for ease of application of transfer-matrix (TM) or recursive Green's functions methods[7,8,9,10,11,13,15,16,17,19]; extrapolation to bulk behavior ($d = 2$ or 3 as the case may be) is then performed with help of finite-size scaling theory[21].

Here we consider TM methods, applied both to strictly one-dimensional systems and to strips of a square lattice. Traditionally the TM approach has been used to calculate Lyapunov exponents (directly related to the localization length of SPST)[7,22], and quantities obtainable from such exponents, e.g., conductances[23,24]. In Sec. II we recall how wavefunction amplitudes may be estimated in the TM context, and illustrate our approach in the simple $d = 1$ case by rederiving the corresponding distributions

found in Ref. 20. In Sec. III, an analogous treatment is developed for strips of a two-dimensional square lattice, and numerical results are displayed and discussed. Conclusions and final remarks are given in Sec. IV.

II. METHOD AND ONE-DIMENSIONAL ILLUSTRATION

We consider the site-disordered Anderson model, for which the tight-binding Hamiltonian is written as

$$\mathcal{H} = \sum_i \varepsilon_i |i\rangle \langle i| + V \sum_{\langle i,j \rangle} |i\rangle \langle j| \quad , \tag{1}$$

where the site self-energies ε_i are independent, identically distributed random variables obeying a specified distribution, $\langle i,j \rangle$ denotes nearest-neighbor sites on a regular lattice, and the energy scale is set by the hopping matrix element, $V \equiv 1$. Disorder intensity is given by the width W of the self-energy probability distribution, taken here as rectangular (same as in Ref. 20):

$$P(\varepsilon_i) = \begin{cases} \text{constant} & -W/2 \le \varepsilon_i \le +W/2 \\ 0 & \text{otherwise} \; . \end{cases} \tag{2}$$

In the TM approach[7], one considers the Hamiltonian Eq. (1) on a quasi-one dimensional $L^{d-1} \times N$ system, $N \gg L$. Denoting by $k = 1, \ldots, N$ the successive cross-sections, and $i = 1, \ldots L^{d-1}$ the respective positions of sites within each cross-section, an electronic wave function at energy E is given in terms of its local amplitudes, $\{\, a_{ik}(E) \,\}$, and tight-binding orbitals $|ik\rangle$, as:

$$\Psi_E = \sum_{ik} a_{ik}(E) \, |ik\rangle \; . \tag{3}$$

With a corresponding change of notation, Eq. (1) reads:

$$\mathcal{H} = \sum_{ik} \varepsilon_{ik} \, |ik\rangle \langle ik| + \sum_{\langle ik, i'k' \rangle} |ik\rangle \langle i'k'| \quad , \tag{4}$$

where $\langle ik, i'k' \rangle$ stands for nearest-neighbor pairs. Applying Eq. (4) to Eq. (3) gives the recursion relation

$$a_{i,(k+1)} = (E - \varepsilon_{ik}) \, a_{ik} - a_{i,(k-1)} - \sum_{i'} a_{i',k} \quad , \tag{5}$$

where i' denotes nearest neighbors of i within the same cross-section (the E-dependence is omitted for clarity). In matricial form,

$$\begin{pmatrix} \psi_{k+1} \\ \psi_k \end{pmatrix} = \begin{pmatrix} P_k & -I \\ I & 0 \end{pmatrix} \begin{pmatrix} \psi_k \\ \psi_{k-1} \end{pmatrix} \; , \; \psi_k \equiv \begin{pmatrix} a_{1,k} \\ a_{2,k} \\ \cdots \\ a_{L^{d-1},k} \end{pmatrix} \tag{6}$$

where, considering, e.g., periodic boundary conditions across the $d-1$ transverse directions[7],

$$P_k = \begin{pmatrix} E - \varepsilon_{1,k} & -1 & 0 & \cdots & -1 \\ -1 & E - \varepsilon_{2,k} & -1 & \cdots & 0 \\ \cdots & \cdots & & & -1 \\ -1 & 0 & \cdots & -1 & E - \varepsilon_{L^{d-1},k} \end{pmatrix} \; . \tag{7}$$

The $(2L^{d-1} \times 2L^{d-1})$ matrix $T_k \equiv \begin{pmatrix} P_k & -I \\ I & 0 \end{pmatrix}$ is symplectic, that is, its eigenvalues occur in pairs $\{\alpha_i, \alpha_i^{-1}\}$, $i = 1, \ldots, L^{d-1}$. As explained at length in Refs. 7,9,13,22, the matrix product $M_N = \prod_{k=1}^{N} T_k$ gives rise to the eigenvalues $\exp \gamma_1 \; \ldots \; \exp \gamma_{L^{d-1}}$, where the γ_i are the Lyapunov characteristic exponents (LCE) for the problem, setting the asymptotic divergence of the corresponding eigenvectors v_i. Being a product of symplectic matrices, M_N also has this property, therefore the LCE occur in symmetric pairs $\{\gamma_i, -\gamma_i\}$. Attention usually concentrates on the LCE of smallest modulus, $\gamma_{L^{d-1}}$, whose inverse gives the longest decay length (identified with the localization length of the Anderson problem).

To see the meaning of the eigenvectors v_i, recall that the physically acceptable (non-diverging) wave function is the one associated with the *negative* LCE of smallest modulus, $\gamma_{L^{d-1}+1}$[25]; the corresponding tight-binding amplitudes $\{a_{ik}^{(L^{d-1}+1)}\}$ will give information on the shape of the electronic wave function of interest (because of the symplectic character of the TM, one might equally consider the *inverse* of the amplitudes associated to $\gamma_{L^{d-1}}$; however, in practice the amount of calculational effort is the same either way) . Little use appears to have been made of this property in the context of TM studies of Anderson localization, except for a calculation of lateral transport properties in layered media[26].

It is important to recall that the site amplitudes are not the directly relevant quantities in the TM approach; instead, in the quasi-one dimensional systems used here the wavefunction decay rate must be defined by comparing the moduli of suitable vectors, each with $2L^{d-1}$ components[7,9,13].

We now take strictly one-dimensional systems, and illustrate how the above ideas work. The matrices T_k are 2×2, and the relevant LCE is γ_2; the corresponding wavefunction amplitude at site k is $a_k^{(2)}$. Starting with an arbitrary pair of states at neighboring sites, say $(a_0, a_1) = (1, 1)$, we first iterate Eq. (6) a number $N_{\rm in}$ of times, taking care to orthonormalize the resulting vectors every $N_{\rm ortho}$ steps (typically, $N_{\rm in} = 100$; we have used $N_{\rm ortho} = 1$, but other authors have used $N_{\rm ortho} \simeq 10$ apparently without noticeable deterioration of results[13,22]). With such initialization the starting vectors are rotated in Hilbert space towards the asymptotic direction of the eigenvectors of M_N. Having done this, we rename the current site as the origin. Recalling from Eq. (6) that the vectors being iterated involve both ψ_k and ψ_{k+1}, one sees that the appropriate quantities to keep track of are the $b_k^{(2)} \equiv \{[a_k^{(2)}]^2 + [a_{k+1}^{(2)}]^2\}^{1/2}$. One might visualize

the process as follows: starting from the pair of site amplitudes (a_0, a_1), one iteratively obtains the pair (a_1, a_2) and so on, until (after r iterations of T) one gets the pair (a_r, a_{r+1}). This latter is legitimately said to be at a distance r from the origin, that is, from the original pair of sites.

We then start to accumulate the products of successive amplitudes $b_k^{(2)}$ at each $N_{\rm ortho}$ steps (*after* orthogonalization, but *before* normalization). At distance r from the new origin, the (relative) wavefunction amplitude is given by

$$A(r) \equiv -\ln \frac{\psi'(r)}{\psi'(0)} = -\sum_{k=1}^{r} \ln b_k^{(2)} \ , \qquad (8)$$

where the notation of Ref. 20 is used for ease of comparison, $\psi'(k) \equiv \{[\psi_k]^2 + [\psi_{k+1}]^2\}^{1/2}$, and the fact that we always make $N_{\rm ortho} = 1$ has been taken into account. In order to generate statistics of the $A(r)$ for a set of distances $\{r_1 < r_2 < \cdots < r_{\rm max}\}$, one iterates the TM for $N_0 \geq r_{\rm max}$ steps, collecting data at the specified points; to collect the next sample, it suffices to keep iterating for another N_0 steps, with no need to reinitialize the wave functions, and so on. After a total of $N_{\rm in} + N_{\rm s}\, N_0$ iterations of the TM, one has $N_{\rm s}$ samples of the $A(r)$ for each distance of interest, The corresponding histograms $H(A, r)$ for $E = 0$, disorder strength $W = 1.0$, $r = 1600$, 3200, and 4800, and $N_{\rm s} = 10^5$ are shown in Fig. 1. These values of the parameters were chosen in order to enable comparison with the exact diagonalization results displayed in Figure 1 of Ref. 20. Indeed, one finds excellent visual agreement between the respective data sets. Numerical analysis of the first three moments of our histograms shows that: (i) for all three distances, they are well-fitted by gaussians of the form

$$H(A, r) = \left(\frac{\lambda}{\pi \sigma r}\right)^{1/2} \exp\left[-\frac{(A - r/\lambda)^2}{\sigma r/\lambda}\right] \ , \qquad (9)$$

with $\sigma \simeq 2.08$, $\lambda \simeq 104$, which are in rather good agreement with the expected values from SPST[20,27] in the limit $N_{\rm s}, r \to \infty$, respectively $\sigma = 2$, $\lambda = 105.045/W^2$; and (ii) the dimensionless skewness S, defined as[28]:

$$S \equiv \left\langle \left(\frac{x - \langle x \rangle}{\Delta}\right)^3 \right\rangle \qquad (10)$$

for a distribution with mean $\langle x \rangle$ and dispersion Δ, has the following values: $S = 0.0250$, 0.0190, 0.0128 respectively for $r = 1600$, 3200, 4800.

Point (ii) is further indication that the wavefunction amplitude distribution indeed approaches a log-normal shape (zero skewness), but only as $r \to \infty$. The approximate dependence on r may be inferred as $S \sim r^{-1/2}$, from the 3 data just quoted.

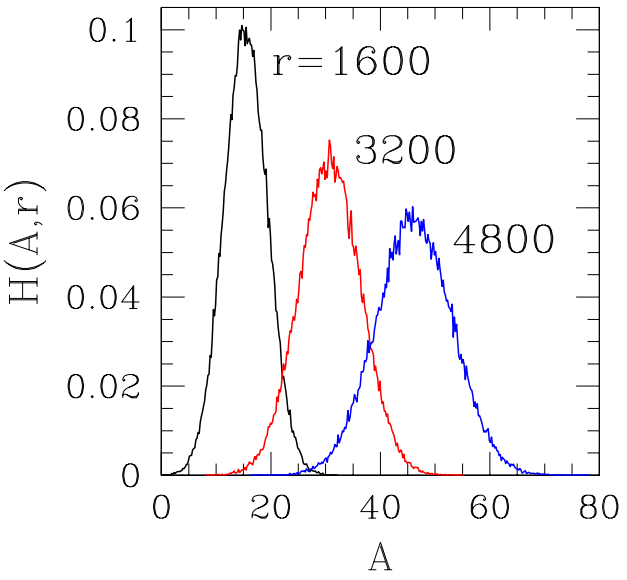

Figure 1: Normalized histograms of occurrence of the logarithmic decay factor, $A(r)$ of Eq. (8), in $d = 1$, for $E = 0$, $W = 1.0$, and distances r as shown. $N_{\rm s} = 10^5$ samples were collected, for each r (see text).

III. STRIPS OF A TWO-DIMENSIONAL LATTICE

We now extend our approach to strips of a square lattice. For a strip of width L, the matrices T_k are $2L \times 2L$, and the relevant LCE is γ_{L+1}; the corresponding wavefunction amplitudes at column k are $a_{ik}^{(L+1)}$, $i = 1, \ldots, L$. Taking into account the normalization of Eq. (6), the appropriate decay factor here is

$$A(r) = -\sum_{k=1}^{r} \ln \left(\sum_{j=k}^{k+1} \sum_{i=1}^{L} \left[a_{ij}^{(L+1)} \right]^2 \right)^{1/2} \qquad (d = 2). \qquad (11)$$

It must be stressed that Eq. (11) is not meant to imply an averaging process over site amplitudes $a_{ij}^{(L+1)}$; as remarked above, these $2L$ quantities are not the directly relevant ones. Instead, they give the modulus of the eigenvector associated to the negative LCE of smallest absolute value[25], whose decay is to be followed.

We have considered strips of even widths $4 \leq L \leq 64$ sites and periodic boundary conditions across, and taken the disorder intensity $W = 10$, in order to make contact with analogous results in Ref. 20. For this value of W SPST predicts the localization length to be $\lambda \simeq 5.45$[9]. SPST, together with finite-size scaling[21] would imply that

$$H(A, r, L, W) = f\left(A, \frac{r}{L}, \frac{r}{\lambda}\right) \ . \qquad (12)$$

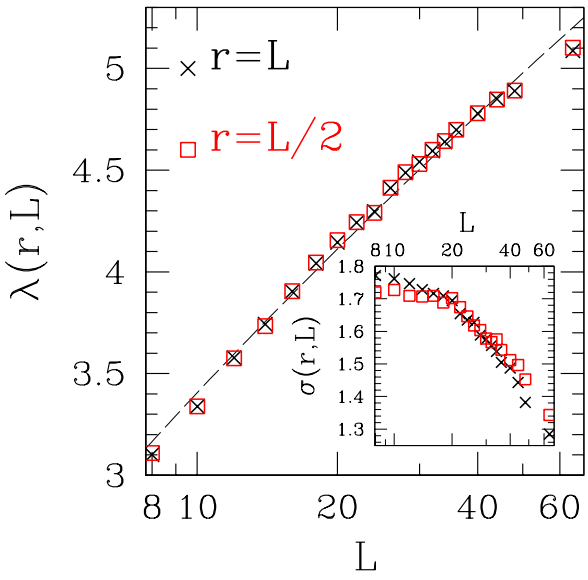

Figure 2: Effective localization lengths on strips of $d = 2$ lattice, fitted from first and second moments of distributions to the gaussian form, Eq. (9), for $E = 0$, $W = 10.0$. Strip widths L and distances r as shown. $N_s = 5 \times 10^4$ samples for $L \leq 40$, 2×10^4 otherwise. Dashed line is $\lambda = 3.4\,(\log L)^{0.72}$ (see text). Scale is logarithmic on horizontal axis. Inset: width of distribution, σ, as defined in Eq. (9). Axis scales and symbols as in main Figure.

In order to infer the $d = 2$ behavior, one must consider the regime $r,\, L \gg 1$, $r/L \lesssim 1$[21]. Although TM methods make it easy to explore long distances ($r \gg L$) along the "infinite" direction, this fact is not directly relevant here, as the corresponding regime would be one where strictly one-dimensional features emerge.

In the following, we shall restrict ourselves to $r/L = 1/2$ and 1; according to Eq. (12), for each value of r/L one should then be able to collapse all distributions against r/λ.

Again, we have examined the first three moments of the distributions thus generated. Using only the first two, we have fitted data to gaussians in the manner of Eq. (9), for which the effective localization lengths $\lambda(r, L)$ are displayed in Fig. 2. It can be seen that, for given L, the λ are essentially the same both for $r = L/2$ and L. This shows that crude finite-size distortions do not play a role for the ranges of r and L used. On the other hand, similarly to the findings of Ref. 20 and against the prediction of SPST, there is no single value of λ to fit all distributions; instead, it grows with increasing r. However, our result differs from that of Ref. 20, in that the dependence of λ is clearly not linear in $\log L$. This should not be seen as a direct contradiction, as the quantities under study are not identical (as was the case in $d = 1$): though they represent the same physical phenomenon of wavefunction decay, they do so in rather different geometries.

As regards the width of distribution σ (again taking Eq. (9) as a starting point) our results, displayed in the inset of Fig. 2, exhibit numerical values not unlike those found in Ref. 20, in the sense of being consistently smaller than the SPST prediction $\sigma = 2$, but with the same order of magnitude. One might expect that, for larger r, L the decreasing trend observed for $20 \lesssim L \lesssim 60$ would stabilize close to $\sigma \simeq 1.3$ quoted in Ref. 20. This, however, we have no means to ascertain at present.

We have not been able to fit the full range of data by a single power of either L or $\log L$; assuming, e.g., $\lambda \sim (\log L)^x$, the best result from a nonlinear least-squares fit gives $x \simeq 0.72$, corresponding to the dashed line in Fig. 2. It is evident, from the Figure, that the trend for large L is towards an even slower variation.

At this point, one might speculate that λ, as given by the gaussian fits, could eventually saturate for larger L, at a value which might even be close to the SPST prediction. However, we shall now show that the gaussian fits themselves become increasingly unable to reflect the properties of the wavefunction amplitude distributions.

Indeed, we have found that the skewness of distributions is negative, and *increases* in absolute value as r, L grow. As an example, Fig. 3 shows the raw data for $L = 48$, $r = 24$, together with the corresponding gaussian fit of Eq. (9), obtained using the first and second moments of the distribution. The effect of negative skewness is apparent in that the gaussian approximation overshoots the data for large A (i.e., predicts a *small* amplitude to occur *more frequently* than observed in fact), and undershoots for small A (predicts a *large* amplitude to occur *less frequently* than observed).

Skewness data for the ranges of r and L used here are displayed in Fig. 4, together with fits of single-power forms, $-S \sim L^x$, for the subsets corresponding respectively to $r = L$ (dashed line, $x \simeq 0.29$) and $r = L/2$ (full line, $x \simeq 0.25$). Despite the large amount of scatter, the increasing trend against growing r, L is unmistakably present. This means, in turn, that for larger and larger systems the distributions become ever less amenable to fitting by gaussians, as predicted by SPST. This would remain true even if a hypothetical saturation should occur for values of r and L larger than those investigated here.

Recall, from Eq. (10), that skewness is invariant under the usual histogram-collapse rescaling[20], $H_s(A_s, r) = H(A, r)\sqrt{\pi\sigma r/\lambda(r)}$, where the shifted variable is $A_s \equiv [A - r/\lambda(r)]\,/\sqrt{\sigma r/\lambda(r)}$. Therefore, this is a legitimate extra parameter to characterize the distributions. Similar results were found experimentally, for the conductance distribution in quasi-one dimensional gold wires[29].

Negative skewness of wavefunction amplitude distributions works in the same way as (in the limited context of gaussian fits) does the finding that $\lambda(r)$ increases with r: both contribute to a slower decay of electronic wave functions, compared with the constant-λ, zero-skewness,

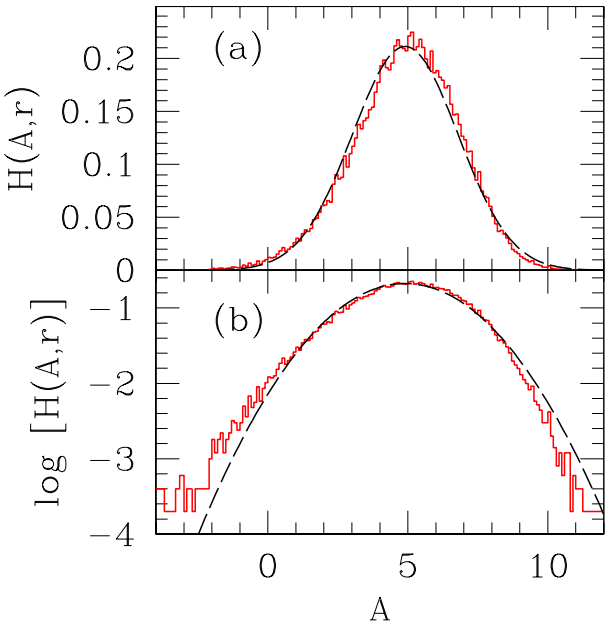

Figure 3: Normalized histogram of occurrence of $A(r)$ of Eq. (11) for $E = 0$, $W = 10.0$, $L = 48$, $r = 24$ (full line). Skewness$=-0.288$. Dashed line: Gaussian fit (Eq. (9)), using first and second moments of distribution. Vertical scale is linear in (a), and logarithmic in (b), the latter in order to emphasize discrepancies between data and fit at the extremes.

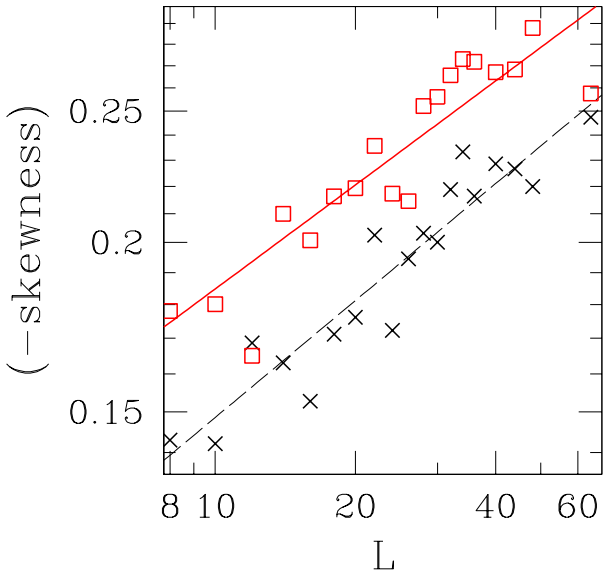

Figure 4: Double-logarithmic plots of negative skewness of wavefunction amplitude distributions, $A(r)$ of Eq. (11), for $E = 0$, $W = 10.0$ against strip width L, and corresponding least-squares fits to single-power forms. Crosses and dashed line: $r = L$. Squares and full line: $r = L/2$.

SPST picture. Of course, the evidence just presented is not enough to argue that there must be a localization-delocalization transition in $d = 2$; the idea that this is the borderline dimensionality, as predicted by SPST, most likely holds true. Nonetheless, we have shown robust evidence for deviations from SPST in $d = 2$, whose consequences still have to be worked out in full,

IV. CONCLUSIONS

We have made use of suitable properties of the vectors which are iterated in the TM approach to Anderson localization[7,9,13,22], in order to generate the statistical distribution of electronic wavefunction amplitudes at sites of $L^{d-1} \times \infty$ disordered systems. We have considered $d = 1$ (for which our approach is shown to reproduce the exact diagonalization results of Ref. 20), and $d = 2$. In the latter case, since the $L \times \infty$ geometry of our systems differs from that $(L \times L)$ of Ref. 20, a perfect match is not to be expected; however, some basic physical properties are found to hold for both cases. In particular, attempted fits of gaussian (log-normal) forms to the wavefunction amplitude distributions result in effective localization lengths growing with distance, contrary to the SPST prediction. We have gone further, and shown that the distributions possess a negative skewness, which is invariant under the usual histogram-collapse rescaling, and increases with distance (at least for the range of parameters used in our study).

Such deviations from the expected behavior are evidence of slower decay of electronic wavefunctions than predicted by SPST; it still must be worked out whether or not some phenomena specific to $d = 2$, such as weak localization, or the recently-observed metal-insulator transition in dilute two-dimensional dilute electron-hole systems[4], carry the fingerprints of the anomalies reported here. We expect that the present results may motivate further work along these lines.

Acknowledgments

Research of S.L.A.d.Q. is partially supported by the Brazilian agencies CNPq (Grant No. 30.1692/81.5), FAPERJ (Grants Nos. E26–171.447/97 and E26–151.869/2000) and FUJB-UFRJ.

[*] Electronic address: sldq@if.ufrj.br

[1] P. W. Anderson, Phys. Rev. **109**, 1492 (1958).

[2] E. Abrahams, P. W. Anderson, D. C. Licciardello, and T. V. Ramakrishnan, Phys. Rev. Lett. **42**, 673 (1979).

[3] A. MacKinnon and B. Kramer, Rep. Prog. Phys. **56**, 1469 (1993).

[4] For a review, see E. Abrahams, S. V. Kravchenko, and M. P. Sarachik, Rev. Mod. Phys. **73**, 251 (2001).

[5] Y. Meir, Phys. Rev. Lett. **83**, 3506 (1999); Phys. Rev. B **61**, 16 470 (2000).

[6] See, e.g., R. Berkovits, J. W. Kantelhardt, Y. Avishai, S. Havlin, and A. Bunde, Phys. Rev. B **63**, 082192 (2001) and references therein.

[7] J.-L. Pichard and G. Sarma, J. Phys. C **14**, L127 (1981); **14**, L617 (1981).

[8] A. MacKinnon and B. Kramer, Phys. Rev. Lett. **47**, 1546 (1981).

[9] A. MacKinnon and B. Kramer, Z. Phys. B: Condens. Matter **53**, 1 (1983).

[10] B. Bulka, B. Kramer, and A. MacKinnon, Z. Phys. B Condens. Matter **60**, 13 (1985).

[11] B. Bulka, M. Schreiber, and B. Kramer, Z. Phys. B Condens. Matter **66**, 21 (1987).

[12] T.-M. Chang, J. D. Bauer, and J. L. Skinner, J. Chem. Phys. **93**, 8973 (1990).

[13] A. McKinnon, J. Phys.: Condens. Matter **6**, 2511 (1994).

[14] J. L. Cardy, *Scaling and Renormalization in Statistical Physics* (Cambridge University Press, Cambridge, 1996), Chap. 3.

[15] K. Slevin and T. Ohtsuki, Phys. Rev. Lett. **82**, 382 (1999).

[16] T. Ohtsuki, K. Slevin, and T. Kawarabayashi, Ann. Phys. (Leipzig) **8**, 655 (1999).

[17] K. Slevin, T. Ohtsuki, and T. Kawarabayashi, Phys. Rev. Lett. **84**, 3915 (2000).

[18] K. Slevin, P. Markos, and T. Ohtsuki, Phys. Rev. Lett. **86**, 3594 (2001).

[19] S. L. A. de Queiroz, Phys. Rev. B **63**, 214202 (2001).

[20] J. W. Kantelhardt and A. Bunde, Phys. Rev. B **66**, 035118 (2002).

[21] M. N. Barber, in *Phase Transitions and Critical Phenomena*, edited by C. Domb and J. L. Lebowitz (Academic, New York, 1983), Vol. 8.

[22] A. Crisanti, G. Paladin, and A. Vulpiani, in *Products of Random Matrices in Statistical Physics*, Springer Series in Solid State Sciences Vol. 104, edited by Helmut K. Lotsch (Springer, Berlin, 1993).

[23] J.-L. Pichard, J. Phys. C **19**, 1519 (1986).

[24] J.-L. Pichard and G. André, Europhys. Lett. **2**, 477 (1986).

[25] F. Delyon, Y. E. Lévy and B. Souillard, Phys. Rev. Lett. **55**, 618 (1985); B. Souillard, in *Chance and Matter, Les Houches Session XLVI*, edited by J. Souletie, J. Vannimenus and R. Stora (Amsterdam: North-Holland, 1987), pg. 305.

[26] M.-C. Chan and Z.-Q. Zhang, Phys. Rev. B **56**, 36 (1997).

[27] M. Kappus and F. Wegner, Z. Phys. B: Condens. Matter **45**, 15 (1981).

[28] W. Press, B. Flannery, S. Teukolsky, and W. Vetterling, *Numerical Recipes in Fortran, The Art of Scientific Computing*, 2nd ed. (Cambridge University Press, Cambridge, 1994), Sec. 14.1.

[29] P. Mohanty and R. A. Webb, Phys. Rev. Lett. **88**, 146601 (2002).